

The influence of strainer types on the flow and droplet velocity characteristics of ceramic flat-fan nozzles

Bahadır SAYINCI*

Department of Agricultural Machinery and Technologies Engineering, Faculty of Agriculture, Atatürk University, Erzurum, Turkey

Received: 26.11.2014

Accepted/Published Online: 18.02.2015

Printed: 00.00.2015

Abstract: This study focused on determining the effect of various strainer types and their usage without strainer on the flow and droplet velocity characteristics of ceramic flat-fan nozzles. The nozzle types discussed are the standard (APE), low pressure drift reduction (ADI), and wide pressure range (AXI). The results of this study show that the orifice coefficient (k) of the ADI nozzle with a preorifice was lower than those of the API and AXI nozzles. The ball check strainers had a limiting effect on the nozzle's flow rate. The pressure exponent coefficients (n) were 0.57 for the API nozzle and 0.62 for the ADI and AXI nozzles used with ball check strainers. The n coefficient ranged from 0.47 to 0.49 for the API and AXI nozzles and from 0.50 to 0.53 for the ADI nozzle, used with typical strainers and without a strainer. The flow rate deviations of APE, ADI, and AXI nozzles used with a ball check strainer were determined as -12.0%, -11.4%, and -14.5%, respectively. The lowest C_d means were found in all nozzle types with ball check strainers, and the means were determined as 0.45, 0.58, and 0.71 for the ADI, AXI, and API nozzles, respectively. The C_d means of the nozzles with typical strainers, which is the same as usage without a strainer, were between 0.58 and 0.60 for the ADI nozzle, 0.82 and 0.85 for the AXI nozzle, and 0.91 and 0.94 for the API nozzle. Knowledge of the discharge coefficient of the nozzles used with various strainer types provided a reasonable estimation of the maximum droplet velocity at the nozzle orifice exit. The maximum droplet velocity at the nozzle orifice exit increased as droplet size increased. The droplets produced by the nozzles with ball check strainers had features that restricted the nozzle's flow. These were higher maximum velocity, kinetic energy, and stopping distance.

Key words: Discharge coefficient, droplet velocity, flat-fan nozzle, flow rate deviation, nozzle strainer, pressure exponent

1. Introduction

The nozzle strainer is one of the most important yet overlooked parts of a sprayer. Usage of nozzle strainers is a necessity for sprayers, since spray nozzles that are used without a strainer on the boom section may lead to clogging of the nozzles, which is a potential problem in pesticide applications. In spray performance, the negative effects of clogging that could cause problems during spraying include decreased flow rate and disturbed spray patterns. Hence, it was indicated by Huyghebaert et al. (2001) that the spray pattern and flow rate of the nozzles are the most crucial properties in spray application, because these variables identify spray performance, spray efficiency, and production quality.

The nozzle strainer type refers to nozzle capacity, and their size is indicated with a mesh unit. The opening of the strainers with high mesh numbers is larger than those with low mesh numbers (Hofman and Solseng, 2004). The strainer mesh size for each nozzle type is recommended in the nozzles' manufacturer catalogues. In general, strainers of 80 or 100 meshes are recommended for most nozzles with a

flow rate below 0.6 L min^{-1} . Strainers of 60 meshes and above are proposed for nozzles with flow rates varying from 0.8 to 3.8 L min^{-1} . No nozzle strainer is needed for nozzles with flow rates of 3.8 L min^{-1} and above if a good line strainer is used. Strainers of 60 meshes and above prevent screen clogging when applied with soluble powder. Finer strainers, of 80 meshes and above, can be used to protect small nozzles when applying liquid concentrates, emulsions, and wettable powders. Small-capacity nozzles should have a strainer of the necessary size to stop any particle from clogging the nozzle orifice. These strainers vary in size, depending on the nozzle capacity used, and are typically 60 and 80 meshes (Lechler GmbH, 2004) or 50 and 100 meshes (Agrotop GmbH, 2010) for nozzle flow rates that range from 0.4 to 3.0 L min^{-1} . A nozzle strainer and check valve combination were designed with the aim of stopping the formation of drip at the exit orifice of a nozzle after spraying. The mesh numbers of strainers with check valves ranged from 24 to 200 meshes. The minimum spray pressure of strainers with check valves was reported as 0.5 bar. Specifically, spraying begins after attaining a pressure level of 0.5 bar.

* Correspondence: bsayinci@atauni.edu.tr

The nozzle flow rate is proportional to the square root of the spray pressure, the exponent (n) of which is 0.50, and this coefficient is accepted as a common value for most nozzle types. However, for some nozzles, the exponent coefficient has been indicated as lower than its common value (Spraying Systems Co., 2014). Undoubtedly, nozzle geometry based on design attributes is a factor affecting the flow characteristics of the nozzle. Furthermore, Sayıncı (2014) determined that the nozzle strainer types influenced the flow characteristics of the flat-fan nozzles, and the exponent coefficient calculated by using a power regression model was found different from the common value of 0.50. Therefore, nozzle strainers that cause a deviation of the exponent coefficient of the spray pressure may also affect nozzle capacity. It is also noted that nozzle tests of quality and availability are implemented without a strainer according to the manufacturer's standards (ASABE, 2009).

In general, it is known that strainers cause local losses in hydraulic systems (Sayıncı, 2014). These local losses in the nozzle systems are represented as a discharge coefficient, which is the ratio of the actual discharge to the theoretical discharge. Most research involves the nozzle discharge coefficient (Lienhard, 1984; Ballester and Dopazo, 1994; Halder et al., 2004; Iqbal et al., 2005; Hussein et al., 2012; Rashid et al., 2012; Sayıncı et al., 2013; Yu et al., 2013). Most research showed that the discharge coefficient of flat-fan nozzles is considerably higher than the disk-core type hollow cone nozzle. Yu et al. (2013) efficiently explained the parameters depending on the discharge coefficient of a nozzle based on some important references. These parameters were indicated as flow regime based on Reynolds number, nozzle geometry, pressure difference, back pressure, and cavitation as attributed to Lefebvre (1989). However, in general broad scanning, there is lack of relevant research about the discharge coefficient of nozzles used with a strainer.

Nozzle capacity provided by the manufacturer is one of the basic parameters used for the field calibration of a sprayer (ASABE, 2012) and is necessary for the fulfilment of quality standards. Strainers may not be used to test the quality standards of the nozzles, but their usage is inevitable in field conditions. Furthermore, it has been determined that the strainers lead to a deviation in the nominal flow rate of the flat-fan nozzles (Sayıncı, 2014).

The aim of this study was to compare the flow and droplet characteristics of the flat-fan ceramic nozzle types used with different types of strainers. The flow characteristics included orifice coefficient, pressure exponent, discharge coefficient, and the individual flow rate deviation of a nozzle, while droplet size, terminal and maximum velocity of droplets, kinetic energy of droplets, stopping distance of droplets, and their drift potential,

estimated using numerical equations, were evaluated in the scope of droplet characteristics.

2. Materials and methods

2.1. Spray nozzles

The spray nozzles used in the present study and their specifications are shown in Table 1. As seen in Figure 1, technical dimensions such as length (L) and width (W) were measured with a stereo zoom microscope (Olympus SZ60, Japan) equipped with a micrometer and digital camera (Panasonic Lumix DMC-FZ50, Japan). After capturing orifice images, the projected area (PA) of the exit orifice and the angle of the V-shaped channel were determined with image processing software SigmaScan Pro v.5.0 and ImageTool v.1.28 (CMEIAS, USA).

As all nozzle bodies were manufactured from thermo-plastic, POM, their orifice bodies were manufactured from ceramic material separately from the nozzle body. The fan spray angle of all nozzles was 110°. Low pressure drift reduction flat-fan nozzles had a ceramic flat preorifice disk of 1 mm in thickness, and an O-ring was used between the ceramic orifice body and preorifice disk to provide impermeability.

Antidrift (ADI; Albus, France) nozzles of a nominal size from 015 to 03 were used for testing. The ADI nozzle had a round preorifice and an elliptical exit orifice. The nozzle body was made of thermo-plastic material, while the exit orifice and round preorifice were manufactured from ceramic material. Standard flat-fan nozzles (APE; Albus) with elliptical orifices, used widely in pesticide applications, had a nominal size of 015 to 03. The API nozzle had a ceramic orifice in a thermo-plastic body. Wide pressure range flat-fan nozzles (AXI; Albus) with a nominal size of 015 to 03 are often used at low pressure in soil applications to reduce spray drift, whereas at high pressure they are used in foliar applications in order to improve target coverage. The recommended pressure ranges from 2 to 4 bar for standard flat-fan nozzles and low pressure drift reduction flat-fan nozzles, and from 1.5 to 2 bar for the wide pressure range flat-fan nozzles (Agrotop GmbH, 2010).




2.2. Nozzle strainers

This study used 2 standard cylindrical strainers with 50-mesh screens of a different type each, 2 screen-type cylindrical strainers of 40 and 80 meshes, 2 ball check strainers of 50 and 80 meshes, 2 slotted strainers of 40 and 50 meshes, and a cup screen type strainer of 50 meshes. The technical properties of the nozzle strainers are given in Table 2.

2.3. Sprayer

A field sprayer (TP 200 Piton, Taral, Turkey) served to perform spray pressures of 1.5, 3.0, 5.0, 7.0, and 10.0 bar. The sprayer had a tank capacity of 200 L and a 6.0-m-wide

Table 1. Technical and operational properties of flat-fan nozzle types.

Technical properties		Standard flat-fan nozzles		
		APE 110015	APE 11002	APE 11003
Nozzle color code		Yellow	Orange	Red
Orifice, major length (L , mm)		1.43	1.55	2.13
Orifice, minor length (W , mm)		0.35	0.55	0.58
V-slot angle (α°)		19°	37°	24°
Entry orifice diameter (D_o , mm)		1.35	1.55	2.13
V-slot height (h , mm)		1.53	1.38	1.47
Orifice, projected area (PA , mm ²)		0.43	0.64	0.96
*Nom. flow rate at 300 kPa spray pressure (L min ⁻¹)		0.61	0.85	1.21
*Droplet size category at 300 kPa spray pressure		F	F	F
		Low pressure drift reduction flat-fan nozzles		
		ADI 110015	ADI 11002	ADI 11003
Nozzle color code		Green	Yellow	Blue
Orifice, major length (L , mm)		1.78	2.12	2.48
Orifice, minor length (W , mm)		0.48	0.54	0.70
V-slot angle (α°)		21°	27°	26°
Entry orifice diameter (D_o , mm)		1.85	2.10	2.50
Preorifice diameter (D_p , mm)		0.83	0.95	1.20
V-slot height (h , mm)		1.49	1.55	1.38
Orifice, projected area (PA , mm ²)		0.69	0.93	1.38
*Nom. flow rate at 300 kPa spray pressure (L min ⁻¹)		0.60	0.80	1.20
*Droplet size category at 300 kPa spray pressure		M	M	M
		Wide pressure range flat-fan nozzles		
		AXI 110015	AXI 11002	
Nozzle color code		Green	Yellow	
Orifice, major length (L , mm)		1.35	1.78	
Orifice, minor length (W , mm)		0.48	0.48	
V-slot angle (α°)		36°	20°	
Entry orifice diameter (D_o , mm)		1.33	1.78	
V-slot height (h , mm)		1.39	1.42	
Orifice, projected area (PA , mm ²)		0.50	0.68	
*Nom. flow rate at 300 kPa spray pressure (L min ⁻¹)		0.60	0.80	
*Droplet size category at 300 kPa spray pressure		F	F	

ˆ: Albuz (2013).

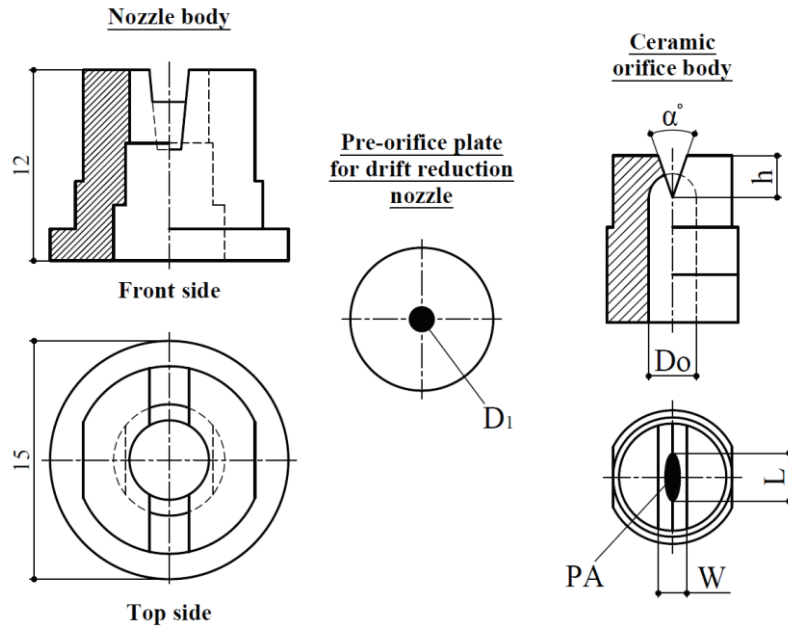


Figure 1. Technical dimensions of flat-fan nozzle types.

spray boom. The sprayer tank was filled with tap water during the trials. The pressure line provided from the exit of the sprayer pump was fitted to a separate line with a triplet nozzle holder manufactured for the trials. To adjust the spray pressure, a pressure regulator (max. 40 bar, 90 L min⁻¹, RG-7 model) was used. The spray pressure was read using a digital manometer (Ref D2, 0.1%, 0–400 bar, Sika GmbH, Germany) located between the nozzle holder and nozzle cap on the dry boom.

The sprayer had a diaphragm-type pump (Tar30 type, flow rate of 30 L min⁻¹ at a pressure of 39.2 bar, Taral) driven with an indicator motor (AGM 100L 4a type, Gamak, Turkey) of 2.2 kW nominal power and 1405 min⁻¹ nominal shaft revolution. A belt-pulley mechanism was used to decrease the rotation of the pump shaft to 500 min⁻¹.

2.4. Flow rate measurements

The flow rates of the nozzles used with different strainer types were determined using a hand-held type of electronic flowmeter (nozzle calibrator, 0.08–3.79 L min⁻¹, ±2.5% accuracy, SC-1 Model, SpotOn, USA) at spray pressure levels of 1.5, 3.0, 5.0, 7.0, and 10.0 bar. The flow rate data were also taken without using strainers. The flow rate measurements were replicated 3 times for each nozzle type, orifice size, strainer type, and operating pressure. Tap water was used during the trials. The sprayer tank was continuously filled to prevent pressure loss in the spray line.

It is indicated that the deviation limit of the nozzle from its nominal capacity ranged within ±10% by the ASABE standards (ASABE, 2012). During the measurements, it

was noted that the individual nozzle flow rate deviation remained between the acceptable limits of ±10%, which is the deviation value from the mean flow rate of a nozzle. Treatments were conducted indoors, where the temperature and relative moisture varied between 13.7 °C and 17.0 °C and between 26% and 29%, respectively.



















2.5. Determination of the orifice coefficient (k) and pressure exponent coefficient (n)

To determine the relation between flow rate (Q) and spray pressure (P) of the nozzle combinations, a power regression model was used ($Q = k \times P^n$; k : orifice coefficient; n : pressure exponent coefficient) (ASABE, 2009). The regression analysis was performed using SPSS 20.0. As the spray pressure factor was treated as an independent variable, the flow rate factor was taken as a dependent variable in the statistical analysis. For each nozzle combination (nozzle type, orifice size, and strainer type), the k and n means were tabulated, and the association of the relation between the flow rate and spray pressure were represented with the determination coefficient (R^2) obtained by the power regression analysis.

2.6. Nozzle flow rate deviation

It is indicated that nozzle flow rate deviation limits range within ±10% in the Turkish standards (Turkish Standards Institution, 2008) and ASABE standards (ASABE, 2012). In this study, Eq. (1) was used to calculate the nozzle flow rate deviation (ϕ) (Huyghebaert et al., 2001). Positive flow rate deviation denoted that the actual flow rate exceeded the nominal nozzle flow rate announced by the manufacturer, while negative marks meant that the measured flow rate was lower than that of the nominal flow rate of the nozzle.

Table 2. Technical properties of the nozzle strainer types.

Strainer types	Mesh size	Screen material	Type	Screen shape	Screen pattern	Screen size (mm)	Strainer images
Cylindrical strainers	40-mesh	Cr-Ni	Screen	Square		0.5 × 0.5	
	50-mesh	Stainless steel	Perforated sheet	Hexagon		0.3 × 0.6**	
	50-mesh	Cr-Ni	Screen	Square		0.3 × 0.3	
	80-mesh	Cr-Ni	Screen	Square		0.2 × 0.2	
Slotted strainers	40-mesh	Brass	Slotted	Slot		6 × 0.5*	
	50-mesh	Brass	Slotted	Slot		8 × 0.3*	
Cup screen type strainer	50-mesh	Stainless steel	Perforated sheet	Circle		Ø 0.6	
Ball check strainers	50-mesh	Cr-Ni	Screen	Square		0.3 × 0.3	
	80-mesh	Stainless steel	Perforated sheet	Hexagon		0.2 × 0.4**	

*: Number of slots × slot opening (mm); **: minor and major lengths of opening-shaped hexagon (mm).

The deviation limits of the flow rate at the confidence interval of 99% were separately tabulated based on the nozzles' orifice sizes and strainer types with regard to the nozzle type.

In order to calculate the nominal flow rate of a nozzle, the flow rate equations of $Q = k \times P^n$ obtained from the power regression model were used. Because the orifice size on a nozzle body, which is stamped by the nozzle manufacturer, is its flow rate at a constant spray pressure of 3.0 bar (300 kPa), the nominal flow rate of a nozzle was determined with regard to its nominal flow rate indicated on the nozzle body in gallons min⁻¹ units. Therefore, the actual flow rate of a nozzle was calculated using power regression equations at a constant spray pressure of 3.0 bar after flow rate measurements.

$$\varphi = \left(\frac{Q_{actual} - Q_{nominal}}{Q_{nominal}} \right) \times 100 \quad (1)$$

2.7. Discharge coefficient

The discharge coefficient (C_d) that depends on the shape of the orifice (Al-Heidary et al., 2014) is defined as the ratio of the actual flow rate to the theoretical flow rate. Hence, C_d is calculated using Eq. (2), which is a general formula regarding the head loss caused by friction in a pipe (Srivastava et al., 1993; Ballester and Dopazo, 1994; Rashid et al., 2012; Yu et al., 2013). The density (ρ_L) of spray liquid at 15 °C, which was measured with a probe-type thermometer positioned near the nozzle orifice outlet during spraying, was determined at 999.1 kg m⁻³.

$$C_d = \frac{Q}{(\Delta P)^{1/n}} \times \left(\frac{\rho_L}{2 \cdot A}\right)^{1/n} \quad (2)$$

2.8. Maximum droplet velocity

The maximum droplet velocity (V_{max}) close to the nozzle exit was calculated based on the nozzle's discharge coefficient using Eq. (3), according to Bernoulli's equation (Al-Heidary et al., 2014).

$$V_{max} = C_d \times \left(\frac{2 \cdot \Delta P}{\rho_L}\right)^n \quad (3)$$

2.9. Prediction of the droplet size of the nozzles used with various strainer types

To estimate the droplet size (volume median diameter, D_{v50}) of APE, ADI, and AXI nozzles, the data from the study of Nuyttens et al. (2007) were referred to and are presented in Table 3. These data were used to calculate the D_{v50} size of the nozzles using Eq. (4) based on their various flow rates at spray conditions of 300 kPa pressure, because the nozzles were operated with various strainer types. The droplet size in Eq. (4), presented by Srivastava et al. (1993), was based on the variation of operating pressure in Pa. This equation was rearranged in order to calculate the D_{v50} size based on the flow rates of the nozzles used with various strainer types.

$$(D_{v50})_2 = (D_{v50})_1 \left(\sqrt[3]{\frac{Q_2}{Q_1}}\right)^n \quad (4)$$

2.10. Terminal velocity of droplet

Stokes' law, which is that the drag force is balanced by friction forces, can be clarified by Eq. (5) (Al-Heidary et al., 2014). It predicts the settling velocity of droplet spheres due to the strength of viscous forces at the surface of the particle providing the majority of the retarding force.

$$V_t = \frac{\rho_d \times g \times D_{v50}^2}{18 \times \mu_a} \quad (5)$$

Substituting the constants related to the liquid temperature of 15 °C and air temperature of 20 °C, V_t within stationary air was obtained as seen in Eq. (6).

$$V_t = (3 \times 10^{-5}) \times D_{v50}^2 \quad (6)$$

2.11. Stopping distance of droplets released in stationary air

The stopping distance (D_s) of droplets released in stationary air was determined using Eq. (7) by Bache and Johnstone (1992), as cited by Nuyttens et al. (2009).

$$D_s = \frac{V_{max} \times D_{v50}^2 \times \rho_d}{18 \times v_a \cdot \rho_a} \quad (7)$$

Substituting the constants related to the liquid temperature of 15 °C and air temperature of 20 °C, D_s could be rearranged as seen in Eq. (8).

$$D_s = (3.041 \times 10^6) \times V_{max} \times D_{v50}^2 \quad (8)$$

2.12. Kinetic energy of the droplets in V_{max}

The kinetic energy (E_k) of the droplets was calculated depending on the maximum velocity attained by the droplets near the nozzle orifice exit and was determined using Eq. (9) (Al-Heidary et al., 2014).

$$E_k = \frac{1}{2} \times \left(\rho_d \times \frac{\pi}{6} \times D_{v50}^3\right) \times V_{max}^2 \quad (9)$$

2.13. Prediction of drift percentage applied volume

Al-Heidary et al. (2014) estimated the drift percentage of the applied volume collected in the wind tunnel versus D_{v50} size of various nozzle types using an exponential equation, [Drift % of applied volume = $31.505 e^{(-0.006 \cdot D_{v50})}$], the determination coefficient of which is 0.93.

2.14. Statistical analysis

Statistical analysis was performed using a completely randomized design. SPSS was used for the analysis of variance with a 95% confidence level (P = 0.05), and Duncan's multiple comparison test was used to determine significant differences. Analysis of variance (ANOVA) tables were constructed and the means and standard deviations were calculated using tabulate.

Table 3. D_{v50} droplet sizes and characteristics of the nozzles, nominal sizes of which are 02 (Nuyttens et al., 2007).

Nozzle types	Nominal flow rate (L min ⁻¹)	D_{v50} (µm)	% volume <100 µm	% volume <200 µm	* V_{vol50} (m/s)
APE 11002	0.80	208.3	8.7	45.9	2.1
ADI 11002	0.80	341.7	2.1	13.2	2.7
AXI 11002	0.78	207.0	9.2	46.6	1.6

*: Velocity of droplets of D_{v50} size at 50-cm sampling distance.

3. Results

3.1. Orifice coefficient

Table 4 shows the relation between nozzle flow rate and spray pressure of the nozzle combination (nozzle type, orifice size, and strainer type). The relation between the 2 variables was explained using the $Q = k \times P^n$ power regression model, and the values with high determination coefficient (R^2) were obtained with regression analysis.

The orifice coefficient (k) increased while the orifice size, which is an indicator of nozzle capacity, increased. Statistically, the k variation of the ADI nozzles compared to the API and AXI nozzles was found to be very significant ($P < 0.01$). As seen in Table 4, the k coefficient of the ADI nozzles with identical orifice sizes was found to be lower than those of the API and AXI nozzles.

The ball check strainers for all nozzle types and orifice size combinations brought about a decrease in nozzle flow rate (Table 4). This finding shows a notable difference among strainer types and is statistically very significant ($P < 0.01$). The k means of the nozzles used with the slotted,

cup screen, and cylindrical strainer types were found to be the same as those with no strainer.

3.2. Pressure exponent coefficient

The pressure coefficient (n) of the nozzle types used in the present study, given in Table 4, was found statistically very significant ($P < 0.01$). The ADI nozzles had higher n means than the API and AXI nozzles. The differences between the n means of the API and AXI nozzles were found insignificant.

In terms of nozzle strainer types, the nozzles with ball check strainers had the highest n means, which were 0.57 for the API nozzle and 0.62 for the ADI and AXI nozzles. The n means of the nozzles used without strainers were the same as those of the slotted, cup screen, and cylindrical strainers. There were no statistical differences between the n means, which ranged from 0.47 to 0.49 for the API and AXI nozzles used with slotted, cup screen, and cylindrical strainers and without strainers. The n means of the ADI nozzles used with other strainers and without a strainer varied between 0.50 and 0.53, except for the ball check type.

Table 4. Relation between the nozzle flow rate (Q) and spray pressure (P) explained with the equation of $Q = k \times P^n$ power regression model (k : orifice coefficient; n : pressure exponent coefficient).

Strainer types	APE 110015			APE 11002			APE 11003			Mean ± SD	
	k	n	R^{2**}	k	n	R^2	k	n	R^2	k	n
No strainer	0.35 ± 0.00	0.49 ± 0.00	0.999	0.48 ± 0.00	0.48 ± 0.00	0.998	0.72 ± 0.00	0.49 ± 0.00	1.000	0.52 ± 0.19 a*	0.49 ± 0.01 b*
Slotted	0.35 ± 0.01	0.50 ± 0.01	0.998	0.49 ± 0.01	0.47 ± 0.01	0.993	0.72 ± 0.00	0.49 ± 0.00	0.999	0.52 ± 0.17 a	0.48 ± 0.02 b
Cup screen	0.35 ± 0.00	0.50 ± 0.00	0.998	0.50 ± 0.00	0.45 ± 0.00	0.998	0.72 ± 0.00	0.49 ± 0.00	0.999	0.52 ± 0.19 a	0.48 ± 0.03 b
Cylindrical	0.36 ± 0.01	0.49 ± 0.01	0.995	0.48 ± 0.01	0.47 ± 0.01	0.998	0.73 ± 0.01	0.48 ± 0.01	0.968	0.52 ± 0.16 a	0.48 ± 0.01 b
Ball check	0.27 ± 0.00	0.61 ± 0.00	0.999	0.41 ± 0.01	0.55 ± 0.01	0.999	0.60 ± 0.07	0.55 ± 0.08	0.981	0.43 ± 0.15 b	0.57 ± 0.05 a
	ADI 110015			ADI 11002			ADI 11003			Mean ± SD	
	k	n	R^2	k	n	R^2	k	n	R^2	k	n
No strainer	0.34 ± 0.00	0.52 ± 0.00	0.998	0.44 ± 0.00	0.52 ± 0.00	1.000	0.70 ± 0.00	0.52 ± 0.00	0.998	0.49 ± 0.19 a	0.52 ± 0.00 b
Slotted	0.33 ± 0.00	0.55 ± 0.02	0.998	0.43 ± 0.00	0.54 ± 0.00	0.999	0.72 ± 0.01	0.49 ± 0.01	0.997	0.50 ± 0.18 a	0.53 ± 0.03 b
Cup screen	0.38 ± 0.00	0.44 ± 0.00	0.983	0.43 ± 0.00	0.53 ± 0.00	0.999	0.71 ± 0.00	0.52 ± 0.00	0.997	0.51 ± 0.18 a	0.50 ± 0.05 b
Cylindrical	0.37 ± 0.02	0.46 ± 0.04	0.985	0.43 ± 0.00	0.54 ± 0.00	0.993	0.71 ± 0.01	0.51 ± 0.02	0.998	0.50 ± 0.16 a	0.50 ± 0.04 b
Ball check	0.26 ± 0.02	0.63 ± 0.07	0.999	0.33 ± 0.03	0.66 ± 0.04	0.998	0.61 ± 0.02	0.57 ± 0.02	1.000	0.40 ± 0.17 b	0.62 ± 0.06 a
	AXI 110015			AXI 11002			Mean ± SD				
	k	n	R^2	k	n	R^2	k	n			
No strainer	0.33 ± 0.00	0.48 ± 0.00	0.999	0.50 ± 0.00	0.48 ± 0.00	0.999			0.41 ± 0.12 a	0.48 ± 0.01 b	
Slotted	0.33 ± 0.00	0.47 ± 0.00	0.999	0.50 ± 0.01	0.48 ± 0.00	0.998			0.42 ± 0.10 a	0.48 ± 0.00 b	
Cup screen	0.35 ± 0.00	0.46 ± 0.00	0.996	0.51 ± 0.00	0.47 ± 0.00	0.999			0.43 ± 0.11 a	0.47 ± 0.01 b	
Cylindrical	0.34 ± 0.01	0.47 ± 0.02	0.990	0.50 ± 0.01	0.48 ± 0.01	0.986			0.42 ± 0.09 a	0.47 ± 0.02 b	
Ball check	0.24 ± 0.01	0.63 ± 0.03	1.000	0.38 ± 0.05	0.60 ± 0.06	0.986			0.31 ± 0.08 b	0.62 ± 0.04 a	

*Means followed by the same letter in the same column are not different at a 5% significance level, as determined by the Duncan test.

** R^2 : Determination coefficient.

3.3. Nozzle flow rate deviation

As seen in Table 5, the flow rate deviation limits of nozzles without a strainer ranged within the acceptable limits of $\pm 10\%$, and the effect of slotted, cup screen, and cylindrical strainers on nozzle flow rate deviation was found to be statistically similar to that of nozzles without a strainer. The flow rate deviation of nozzles with ball check strainers was higher than those of nozzles with other strainers. The flow rate deviation means of the APE, ADI, and AXI nozzles used with ball check strainers was determined as -12.0% , -11.4% , and -14.5% , respectively. Regarding the confidence interval of 99% concerning the flow rate deviation of the nozzles, the flow rate deviation of nozzles with ball check strainers was either within the sublimit of $\pm 10\%$ or exceeded this acceptable deviation limit, as seen in Table 5.

3.4. Discharge coefficient

The results of the ANOVA showed that the nozzle and strainer type had a statistically significant effect ($P < 0.01$) on the variation of discharge coefficient (C_d), while the orifice sizes of the nozzles were of insignificant effect ($P > 0.05$). The highest C_d among the nozzles was found in the API nozzle, as seen in Table 6. The AXI nozzle had the

second highest C_d . It was noted that the ADI nozzle, which is of a low pressure drift reduction type, had the lowest C_d among the flat-fan nozzles.

The lowest C_d level was found in all nozzle types with ball check strainers, and the means were determined as 0.45, 0.58, and 0.71 for the ADI, AXI, and API nozzles, respectively. The C_d means of the nozzles used with slotted, cup screen, and cylindrical strainers were found to be the same as those without a strainer, and the means ranged from 0.58 to 0.60 for the ADI nozzle, 0.82 to 0.85 for the AXI nozzle, and 0.91 to 0.94 for the API nozzle.

3.5. Evaluation of the nozzle types in terms of droplet characteristics and their drift potential

As seen in Table 7, it was noted that the droplets produced with nozzles using ball check strainers, which have a feature restricting nozzle flow, had a higher maximum velocity (V_{max}), kinetic energy (E_k), and stopping distance (D_s), although the droplet size (D_{v50}) decreased for all nozzle types compared to those without a strainer or with typical strainer types. The decreasing D_{v50} resulted in decreasing the terminal velocity (V_t) of the droplets and increasing the drift potential for all nozzle types.

Table 5. The flow rate deviation means of the nozzle types at a spray pressure of 3.0 bar and their confidence interval of 99%.

Strainer types	APE 110015	APE 11002	APE 11003	Mean \pm SD	99% confidence interval	
					Lower bound	Upper bound
No strainer	-0.5	-5.1	1.9	-1.3 ± 3.6 a*	-2.8	0.3
Slotted	-1.1	-4.1	1.7	-1.2 ± 2.6 a	-2.3	-0.1
Cup screen	-1.0	-2.9	2.7	-0.4 ± 2.8 a	-2.0	1.2
Cylindrical	-0.5	-4.8	2.1	-1.1 ± 3.0 a	-1.8	-0.3
Ball check	-14.1	-12.9	-9.0	-12.0 ± 2.6 b	-13.1	-10.9
Strainer types	ADI 110015	ADI 11002	ADI 11003	Mean \pm SD	99% confidence interval	
					Lower bound	Upper bound
No strainer	0.4	-1.6	3.7	0.8 ± 2.7 a	-1.1	2.7
Slotted	2.3	-3.6	3.6	0.8 ± 3.4 a	-1.0	2.1
Cup screen	1.6	-2.9	4.1	0.9 ± 3.6 a	-1.0	2.8
Cylindrical	1.2	-3.4	3.5	0.4 ± 3.1 a	-0.5	1.4
Ball check	-13.2	-16.2	-4.7	-11.4 ± 5.6 b	-12.7	-10.0
Strainer types	AXI 110015	AXI 11002		Mean \pm SD	99% confidence interval	
					Lower bound	Upper bound
No strainer	-7.3	5.5		-0.9 ± 9.0 a	-4.9	3.2
Slotted	-6.7	5.3		-0.7 ± 7.0 a	-3.6	2.2
Cup screen	-4.3	5.9		0.8 ± 7.2 a	-3.3	4.9
Cylindrical	-6.0	5.4		-0.3 ± 6.2 a	-2.3	1.8
Ball check	-20.5	-8.5		-14.5 ± 7.4 b	-17.4	-11.6

*Means followed by the same letter in the same column are not different at a 5% significance level, as determined by the Duncan test.

Table 6. Discharge coefficient (C_d) of the APE, ADI, and AXI flat-fan nozzles used with different types of the strainers with regard to the nozzle orifice sizes (mean \pm SD).

Strainer types	APE 110015	APE 11002	APE 11003	Mean \pm SD
No strainer	0.96 \pm 0.00	0.88 \pm 0.00	0.88 \pm 0.00	0.91 \pm 0.05 a*
Slotted	0.96 \pm 0.02	0.90 \pm 0.02	0.88 \pm 0.01	0.92 \pm 0.04 a
Cup screen	0.96 \pm 0.00	0.95 \pm 0.00	0.89 \pm 0.00	0.94 \pm 0.04 a
Cylindrical	0.98 \pm 0.02	0.89 \pm 0.03	0.89 \pm 0.01	0.92 \pm 0.05 a
Ball check	0.71 \pm 0.00	0.74 \pm 0.03	0.70 \pm 0.07	0.71 \pm 0.04 b
Strainer types	ADI 110015	ADI 11002	ADI 11003	Mean \pm SD
No strainer	0.61 \pm 0.00	0.56 \pm 0.00	0.61 \pm 0.00	0.59 \pm 0.03 a
Slotted	0.57 \pm 0.01	0.54 \pm 0.01	0.63 \pm 0.01	0.58 \pm 0.04 a
Cup screen	0.64 \pm 0.00	0.55 \pm 0.00	0.62 \pm 0.00	0.60 \pm 0.05 a
Cylindrical	0.63 \pm 0.01	0.55 \pm 0.01	0.61 \pm 0.01	0.60 \pm 0.04 a
Ball check	0.43 \pm 0.04	0.40 \pm 0.03	0.52 \pm 0.03	0.45 \pm 0.06 b
Strainer types	AXI 110015	AXI 11002		Mean \pm SD
No strainer	0.76 \pm 0.00	0.87 \pm 0.00		0.82 \pm 0.08 a
Slotted	0.79 \pm 0.00	0.87 \pm 0.02		0.83 \pm 0.05 a
Cup screen	0.82 \pm 0.00	0.89 \pm 0.00		0.85 \pm 0.05 a
Cylindrical	0.80 \pm 0.04	0.87 \pm 0.01		0.83 \pm 0.05 a
Ball check	0.54 \pm 0.03	0.63 \pm 0.08		0.58 \pm 0.07 b

*Means followed by the same letter in the same column are not different at a 5% significance level, as determined by the Duncan test.

Table 7. Prediction of droplet characteristics of the nozzle types used with or without strainers and their drift potential.

Usage of the nozzles with strainers	Nozzle type	Orifice size	$D_{v0.50}$ (μm)	V_{max} (m s^{-1})	E_k (μj)	V_t (m s^{-1})	D_s (m)	Drift (%)
Without strainer or with typical strainers	AXI	015	198.0 \pm 1.9	16.2 \pm 1.0	0.5 \pm 0.1	1.2 \pm 0	1.9 \pm 0.1	9.6 \pm 0.1
	APE	02	201.8 \pm 1.2	18.0 \pm 0.8	0.7 \pm 0.1	1.2 \pm 0	2.2 \pm 0.1	9.4 \pm 0.1
	AXI	02	214.9 \pm 0.9	18.4 \pm 0.4	0.9 \pm 0.0	1.4 \pm 0	2.6 \pm 0.1	8.7 \pm 0.1
	APE	03	211.2 \pm 0.7	20.2 \pm 0.8	1.0 \pm 0.1	1.3 \pm 0	2.8 \pm 0.1	8.9 \pm 0.1
	APE	015	207.3 \pm 1.2	22.5 \pm 0.8	1.2 \pm 0.1	1.3 \pm 0	2.9 \pm 0.1	9.1 \pm 0.1
	ADI	03	349.7 \pm 0.8	16.1 \pm 1.4	2.9 \pm 0.5	3.7 \pm 0	6.0 \pm 0.5	3.9 \pm 0.1
	ADI	015	345.1 \pm 1.9	14.7 \pm 4.4	2.5 \pm 1.5	3.6 \pm 0	5.3 \pm 1.6	4.0 \pm 0.1
Ball check strainers	ADI	02	334.9 \pm 1.6	16.7 \pm 0.4	2.7 \pm 0.1	3.4 \pm 0	5.7 \pm 0.1	4.2 \pm 0.1
	AXI	015	183.3 \pm 0.9	29.6 \pm 3.4	1.4 \pm 0.3	1.0 \pm 0.0	3.0 \pm 0.3	10.5 \pm 0.1
	APE	02	191.4 \pm 1.6	24.2 \pm 0.4	1.1 \pm 0.0	1.1 \pm 0.0	2.7 \pm 0.0	10.0 \pm 0.1
	AXI	02	197.3 \pm 4.5	30.2 \pm 7.9	1.9 \pm 0.8	1.2 \pm 0.1	3.6 \pm 0.8	9.7 \pm 0.2
	APE	03	196.9 \pm 0.9	24.8 \pm 10.2	1.3 \pm 1.0	1.2 \pm 0.0	2.9 \pm 1.1	9.7 \pm 0.1
	APE	015	191.7 \pm 0.2	34.7 \pm 0.3	2.2 \pm 0.0	1.1 \pm 0.0	3.9 \pm 0.0	10.0 \pm 0.0
	ADI	03	332.3 \pm 3.3	19.9 \pm 0.9	3.8 \pm 0.2	3.3 \pm 0.1	6.7 \pm 0.1	4.3 \pm 0.1
ADI	015	317.1 \pm 0.1	25.3 \pm 9.2	5.7 \pm 3.9	3.0 \pm 0.0	7.8 \pm 2.8	4.7 \pm 0.0	
ADI	02	312.5 \pm 4.3	27.1 \pm 4.5	5.9 \pm 1.7	2.9 \pm 0.1	8.1 \pm 1.1	4.8 \pm 0.1	

4. Discussion

4.1. Orifice coefficient

The values with high R^2 regarding the relation between the flow rate and spray pressure of the nozzle combinations (nozzle type, orifice size, and strainer type) were found considerably reliable (Table 4). The k coefficient, referred to as the orifice coefficient by the ASABE standards (ASABE, 2009), is the flow rate to the exponent (n) root of spray pressure. The flow rate differences among the nozzle types at a constant pressure value might represent information about their flow characteristics, manufacturing quality, and applicability to the international standards of the nozzle types based on their design parameter. Thus, the k coefficient might be a comparison variable among the spray nozzle types. Having a low k coefficient means that the nozzle flow rate at a constant pressure value was lower than that of the other nozzle types.

Discharging the lower rate of the ADI nozzle, with a lower k coefficient than the API and AXI nozzle types, depends on its design parameters. The ADI nozzles use a preorifice to reduce the pressure within the nozzle body. These nozzle types are often referred to as drift reduction flat-fan nozzles and produce larger droplets at a constant operating pressure. Due to low pressure, the elliptically shaped orifice area of the ADI nozzle is manufactured larger than that of the standard flat-fan nozzle, as seen in the Table 1.

The ball check strainers had a limiting effect on the flow rate of the nozzles, and this effect was significantly different than the cup screen, slotted, and cylindrical strainers. The ball check strainers are generally used with the aim of preventing the dripping pesticide drops from exiting the orifice of the nozzle after application. A spring and a sphere within the strainer body act as a check valve and open the exit orifice after a pressure value ranging from 0.3 to 2.8 bar (Agrotop GmbH, 2010). This feature of ball check strainers has a restrictive effect on spraying liquid and is an important cause of velocity losses due to the spring resistance (Sayıncı, 2014).

4.2. Pressure exponent coefficient

Typically, the volumetric flow rate of a spray nozzle is proportional to the square root of spray pressure, the exponent coefficient (n) of which is 0.50. However, several findings and the data indicated by the manufacturer for specific nozzle types showed that the n coefficient varied based on nozzle design. Moreover, the present study revealed that the nozzle strainers are able to vary the flow characteristic of the nozzle types.

Spraying Systems Co. (2014) has indicated that the n coefficient is 0.44 for full cone nozzles of wide spray and wide square spray, and 0.46 for full cone nozzles of standard square, oval, and large capacity. Bete Inc. (2014) has also indicated that the n coefficient ranges from 0.43 to 0.47 for most full cone nozzles, and it is 0.50 for most flat-fan industrial nozzles.

In the study conducted by Sayıncı (2014), the n coefficient was determined to vary between 0.48 and 0.49 for standard flat-fan agricultural nozzles manufactured with POM material, while the n coefficient of nozzles with ball check strainers of 50 and 80 meshes was found as 0.55 and 0.57, respectively. The findings of the present study regarding the API ceramic standard flat-fan nozzle were found to be compatible with the data of the previous study. However, it was determined that the ADI drift reduction and AXI wide pressure range nozzles had a higher n coefficient than the API standard flat-fan nozzle (Table 4).

4.3. Nozzle flow rate deviation

Conspicuously, ball check strainers caused the nozzle flow rate to decrease due to their restrictor feature (Table 5). According to the 99% confidence interval of the flow rate deviation, the values exceeded the acceptable limit of $\pm 10\%$ for all nozzle types used in this study. The ball check strainers had a limiting effect on the flow within the strainer body, because the check valve consisted of spring and sphere. Thus, Sayıncı (2014) determined that the flow rate deviation of the standard flat-fan nozzles used with the ball check strainers of 50 and 80 meshes was -11.4% and -12.3% , respectively.

As for the effect of the strainer types on droplet characteristics, the ball check strainers decreased D_{v50} droplet size of the nozzle types compared to nozzles without strainers and those with typical strainers.

4.4. Discharge coefficient

Because the ball check strainers had a limiting effect on the flow of the nozzles, the C_d means were found to be lower than those of the other nozzles. Decreasing the flow rate of a nozzle means that the head losses increase.

The C_d of a nozzle, a significant design parameter, depends on orifice size, orifice shape, and nozzle geometry (Srivastava et al., 1993; Al-Heidary et al., 2014) and explains energy loss from eddies and friction through the exit orifice (Womac and Bui, 2002). It might be suggested that studies concerned with the C_d of agricultural nozzles are considerably limited. However, to determine the orifice size of the nozzle and to predict the drift potential of agricultural nozzles (Sarker and Parkin, 1995, as cited by Çelen and Önlü, 2011), it is necessary to know the C_d of the nozzles.

Womac and Bui (2002) reported that the C_d value for flat-fan nozzles was approximately 0.95 ± 0.02 . Wilkinson et al. (1999) remarked that the C_d of spray nozzles ranged between 0.15 and 0.65. The C_d for disk-core type hollow cone nozzles ranged from 0.14 to 0.61, as indicated by Sayinci et al. (2013). Zhou et al. (1996) stated that the C_d of 10 flat-fan nozzles, the spray angles of which ranged between 15° and 110° , varied from 0.91 to 0.98. It was indicated that the C_d value of the nozzles whose orifices had sharp edges ranged between 0.60 and 0.80 by the ASME (1961).

4.5. Relation between droplet size and maximum droplet velocity

The highest droplet velocity is generally produced close to the nozzle orifice exit and slows down during transport to the target (Al-Heidary et al., 2014). Knowing the discharge coefficient of the nozzles used with various strainer types also provides an estimation of the results closer to the real value.

It is expected that there is a significant correlation between droplet size and velocity. However, it was concluded that there was no correlation between V_{max} at the nozzle orifice exit and D_{v50} droplet size, whereas V_t was compatible with D_{v50} droplet size with reference to the data of Table 7. Furthermore, although it was expected that higher droplet D_{v50} would increase the V_{max} of the droplet at the nozzle orifice exit, the relation between droplet size and droplet velocity is not explicit, as seen in Figure 2. The high variation of droplet velocity within a droplet size interval might be the cause of this uncertainty. The reason of the variation of droplet velocity, resulting in higher

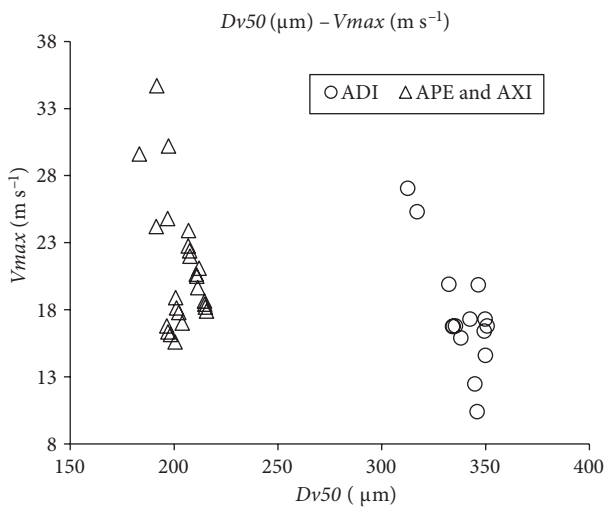


Figure 2. Relation between droplet size (D_{v50}) and maximum droplet velocity (V_{max}).

standard deviation within the droplet size interval, is that droplet velocity is only measured vertically, whereas most droplets have a horizontal velocity component (Nuyttens et al., 2009).

The uncertain relation between droplet size and velocity might also be associated with the low drift nozzle’s design, whose preorifice effect resulted in a pressure drop within the nozzle (Miller, 1999). This pressure drop decreased liquid pressure at the nozzle orifice exit and the proportion of small droplets for low-drift nozzles compared to standard flat-fan nozzles (Nuyttens et al., 2009).

4.6. Kinetic energy and stopping distance of droplets

A significant correlation was seen between the V_{max} of droplets and E_k at the nozzle exit (Figure 3). The droplets produced with an ADI nozzle had higher kinetic energy compared to the APE and AXI nozzle types. At the same spray pressure, the kinetic energy gain of the smaller droplets in D_{v50} was lower than that of the larger droplets. Thus, the ADI nozzle had a higher slope of line compared to the APE and AXI nozzle types, which is seen in Figure 3.

As the E_k of the droplets increased, their D_s also increased in meters under stationary air conditions (Figure 4). There was a highly significant exponential relation with high determination coefficient (R^2) between both parameters. This shows that the droplets produced by the ADI nozzle can be transported over larger distances due to their higher kinetic energy.

4.7. Drift potential of the nozzle types

In Figure 5, the significant relation between the V_t of droplets and their drift potential can be seen. The proportionally low increase of terminal velocity for the

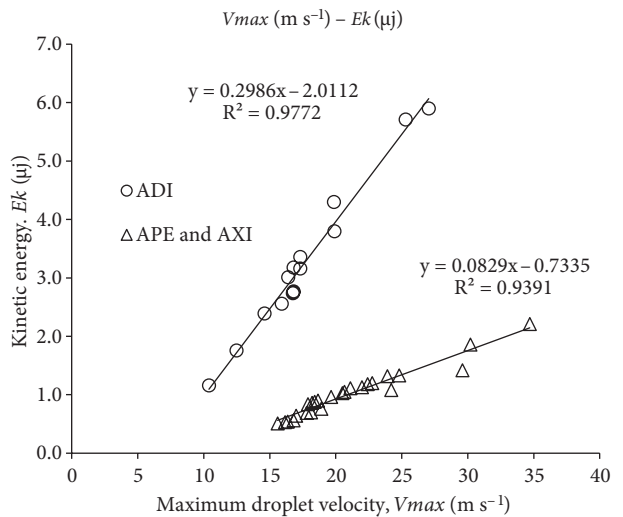


Figure 3. Kinetic energy (E_k) of droplets attaining maximum droplet velocity (V_{max}) at the nozzle orifice exit.

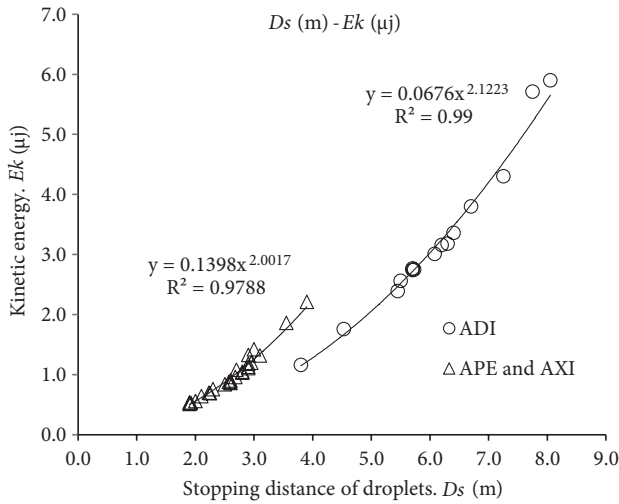


Figure 4. Kinetic energy (E_k) of droplets at stopping distance (D_s) in stationary air.

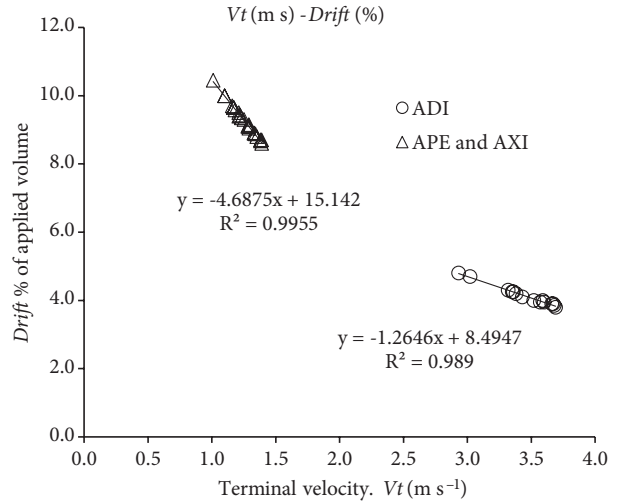


Figure 5. Drift percentage of applied volume versus droplets attaining terminal velocity (V_t).

APE and AXI nozzle types considerably decreased the drift potential of droplets attaining terminal velocity. V_t depends on D_{v50} droplet size produced by the nozzle. Because the V_t

of droplets with large D_{v50} size is higher compared to small droplets, it is significant that the standard flat-fan nozzles are operated at low spraying pressures.

Nomenclature

Φ	nozzle flow rate deviation, %	$(D_{v50})_2$	volume median diameter of the nozzle with Q_2 flow rate, μm
Q_{actual}	actual flow rate of a nozzle, L min^{-1}	$(D_{v50})_1$	volume median diameter of the nozzle with Q_1 flow rate, μm
$Q_{nominal}$	nominal flow rate of a nozzle, L min^{-1}	D_{v50}	volume median diameter of droplet, μm
C_d	discharge coefficient	V_t	terminal velocity of droplet, m s^{-1}
Q	measured flow rate, $\text{m}^3 \text{s}^{-1}$	g	gravitational force of 9.81 m s^{-2}
ΔP	total pressure drop, Pa	μ_a	dynamic viscosity of the air of $1.825 \times 10^{-5} \text{ kg m}^{-1} \text{ s}^{-1}$
ρ_L	liquid density, kg m^{-3}	ρ_d	density of a droplet of 999.1 kg m^{-3}
A	orifice area, m^2	ν_a	kinematic viscosity of the air of $1.516 \times 10^{-5} \text{ m}^2 \text{ s}^{-1}$
n	pressure exponent coefficient	ρ_a	density of the air of 1204 kg m^{-3}
	orifice coefficient (equivalent to coefficient k)	E_k	kinetic energy of the droplet at nozzle orifice exit, j
V_{max}	maximum droplet velocity, which is the initial velocity of a droplet, m s^{-1}		

References

Agrotop GmbH (2010). Spray Nozzles and Accessories for Crop Protection. Product Catalogue, 107/E. Obertraubling, Germany: Agrotop.

Al-Heidary M, Douzals JP, Sinfort C, Vallet A (2014). Influence of nozzle type, nozzle arrangement and side wind speed on spray drift as measured in a wind tunnel. In: Proceedings of the IRSTEA International Conference of Agricultural Engineering, 6–7 July 2014; Zurich, Switzerland. Montpellier, France: National Research Institute of Science and Technology for Environment and Agriculture, pp. 1–7.

Albuz (2013). Spray Nozzles. Product Catalogue. Gravigny, France: Albuz.

ASABE (2009). ANSI/ASAE S572.1: MAR1991. Spray Nozzle Classification by Droplet Spectra. St. Joseph, MI, USA: ASABE.

ASABE (2012). Guide for Preparing Field Sprayer Calibration Procedures. ASAE EP367.2 MAR1991 (R2012). St. Joseph, MI, USA: ASABE.

ASME (1961). Flowmeter Computational Handbook. New York, NY, USA: American Society of Mechanical Engineers.

- Bache DH, Johnstone DR (1992). *Microclimate and Spray Dispersion*. Chichester, UK: Ellis Harwood.
- Ballester J, Dopazo C (1994). Discharge coefficient and spray angle measurements for small pressure-swirl nozzles. *Atomization Spray* 4: 351–367.
- Bete Inc. (2014). *Bete Spray Nozzles, Engineering Information Catalogue*. Greenfield, MA, USA: Bete.
- Çelen IH, Önler E (2011). Reducing spray drift. In: Stoytcheva M, editor. *Pesticides in the Modern World – Pesticides Use and Management*. Rijeka, Croatia: InTech, pp. 149–168.
- Halder MR, Dash SK, Som SK (2004). A numerical and experimental investigation on the coefficients of discharge and the spray cone angle of a solid cone swirl nozzle. *Exp Therm Fluid Sci* 28: 297–305.
- Hansen PD (1993). Chemical application. In: Srivastava AK, Goering CE, Rohrbach RG, editors. *Engineering Principles of Agricultural Machines*. St. Joseph, MI, USA: American Society of Agricultural Engineers, pp. 265–324.
- Hofman VL, Solseng EG (2004). *Spray Equipment and Calibration*. Fargo, ND, USA: North Dakota State University.
- Hussein A, Hafiz M, Rashid H, Halim A, Wisnoe W, Kasolang S (2012). Characteristics of hollow cone swirl spray at various nozzle orifice diameters. *Jurnal Teknologi* 58: 1–4.
- Huyghebaert B, Debouche C, Mostade O (2001). Flow rate quality of new flat fan nozzles. *T ASABE* 44: 769–773.
- Iqbal M, Ahmad M, Younis M (2005). Effect of Reynold's number on droplet size of hollow cone nozzle of environment friendly university boom sprayer. *Pak J Agri Sci* 42: 106–111.
- Lechler GmbH (2004). *Agrardüsen und Zubehör*. Metzingen, Germany: Lechler GmbH.
- Lefebvre AH (1989). *Atomization and Sprays*. New York, NY, USA: Taylor and Francis.
- Lienhard V (1984). Velocity coefficients for free jets from sharp-edged orifices. *J Fluid Eng* 106: 13–17.
- Miller PCH (1999). Factors influencing the risk of drift into field boundaries. In: *Proceedings of the Brighton Crop Protection Conference*, 15–18 November 1999; Brighton, UK. Alton, UK: British Crop Protection Council, pp. 436–446.
- Nuyttens D, Baetens K, De Schampheleire M, Sonck B (2007). Effect of nozzle type, size and pressure on spray droplet characteristics. *Biosyst Eng* 97: 333–345.
- Nuyttens D, De Sphampheleire M, Verboven P, Brusselman E, Dekeyser D (2009). Droplet size and velocity characteristics of agricultural sprays. *T ASABE* 52: 1471–1480.
- Rashid MSFM, Hamid AHA, Sheng OC, Ghaffar ZA (2012). Effect of inlet slot number on the spray cone angle and discharge coefficient of swirl atomizer. *Procedia Eng* 41: 1781–1786.
- Sarker KU, Parkin CS (1995). Prediction of spray drift from flat-fan hydraulic nozzles using dimensional analysis. In: *Proceedings of the Brighton Crop Protection Conference*, 20–23 November 1995; Brighton, UK. Farnham, UK: British Crop Protection Council, pp. 529–534.
- Sayinci B (2014). Effect of filter types and sizes on flow characteristics of standard flat-fan nozzles. *Tarım Makinaları Bilimi Dergisi* 10: 129–138 (article in Turkish with abstract in English).
- Sayinci B, Bozdoğan NY, Yıldız C, Demir B (2013). Determination of discharge coefficient and some operational features of hollow cone nozzles. *Tarım Makinaları Bilimi Dergisi* 9: 9–20 (article in Turkish with abstract in English).
- Spraying Systems Co. (2014). *Industrial Hydraulic Spray Products. Catalogue 75*. Wheaton, IL, USA: Spraying Systems Co.
- Turkish Standards Institution (2008). TS EN 13790-1, *Tarım Makinaları - Pülverizatörler - Kullanımdaki Pülverizatörlerin Muayenesi - Bölüm 1: Tarla Pülverizatörleri*. Ankara, Turkey: TSI (in Turkish).
- Wilkinson R, Balsari P, Oberti R (1999). Pest control equipment. In: Stout BA, Cheze B, editors. *CIGR Handbook of Agricultural Engineering*. Vol. III. St. Joseph, MI, USA: American Society of Agricultural Engineers, pp. 269–310.
- Womac AR, Bui QD (2002). Design and tests of a variable-flow fan nozzle. *T ASABE* 45: 287–295.
- Yu B, Fu PF, Zhang T, Zhou HC (2013). The influence of back pressure on the flow discharge coefficients of plain orifice nozzle. *Int J Heat Fluid Fl* 44: 509–514.
- Zhou Q, Miller PCH, Walklate PJ, Thomas NH (1996). Prediction of spray angle from flat-fan nozzles. *J Agr Eng Res* 64: 139–148.

